THE JOURNAL OF PHYSICAL CHEMISTRY Letters

LETTER

pubs.acs.org/JPCL

Critical Shell Thickness of Core/Shell Upconversion Luminescence Nanoplatform for FRET Application

Yu Wang,[†,‡,§] Kai Liu,[†,‡,§,∥] Xiaomin Liu,[§] Kateřina Dohnalová,[⊥] Tom Gregorkiewicz,[⊥] Xianggui Kong,[*,§] Maurice C. G. Aalders,[∥] Wybren J. Buma,[†] and Hong Zhang[*,†]

[†]van't Hoff Institute for Molecular Sciences, University of Amsterdam, Science Park 904, 1098 XH Amsterdam, The Netherlands

[‡]Graduate School of Chinese Academy of Sciences, Beijing 100039, Peoples Republic of China

[§]Changchun Institute of Optics, Fine Mechanics and Physics, Chinese Academy of Sciences, 3888 Eastern South Lake Road, Changchun 130033, Peoples Republic of China

[∥]Department of Biomedical Engineering and Physics, Academic Medical Center, University of Amsterdam, 1105 AZ Amsterdam, The Netherlands

[⊥]van der Waals-Zeeman Institute, University of Amsterdam, Science Park 904, 1098 XH Amsterdam, The Netherlands

Supporting Information

ABSTRACT: Almost all the luminescence upconversion nanoparticles used for Förster resonant energy transfer (FRET) applications are bare cores based on the consideration that the energy transfer efficiency is optimized because the distance between energy donors and acceptors is minimized. On the other hand, it is well proved that core/shell structure is efficient in minimizing the nonradiative loss of excitation energy of the luminescence donors. In this work we use core/shell upconversion $NaYF_4$:Yb^{3+},Er^{3+}@$NaYF_4$ nanoparticles and rose bengal photosensitizer to construct a FRET conjugate. From the photophysics and singlet oxygen generation we have determined that the core/shell structured nanoparticles are better than bare cores for FRET applications. More importantly, we have found that there exists a critical shell thickness for the best FRET performance. In the model we have established, the critical shell thickness is a trade-off between the opposing optimal conditions for upconversion and FRET efficiency. This work shall lead to more efficient FRET-based applications of nanomaterials.

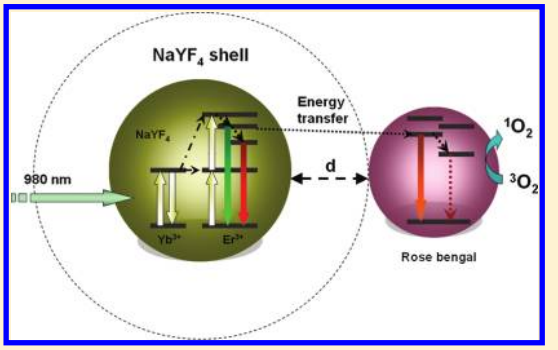

SECTION: Nanoparticles and Nanostructures

Rare earth ion (RE^{3+})-doped upconversion nanoparticles (UCNPs) have recently been introduced as energy donors for Förster resonant energy transfer (FRET)-based applications in biological/biomedical fields.[1−11] FRET is a direct and effective method widely used in bioassays,[12] biosensing and bioimaging,[13,14] and photodynamic therapy.[15−19] In comparison to traditional fluorescent energy donors such as organic dyes and quantum dots, the advantages of UCNPs stem from their unique property of being able to emit multicolor visible light under continuous wave near-infrared (NIR) light. Due to the absence of autofluorescence and reduction of light scattering under such conditions, an excellent signal-to-noise ratio in detection can be obtained. From a biomedical point of view, the use of NIR light is very attractive, since NIR radiation has a higher tissue penetration than normal UV−visible (UV−vis) radiation and leads to less photodamage to living organisms. There is thus a large area of bioapplications where such systems could potentially significantly advance the state of the art.

However, as yet, the poor upconversion quantum yield of UCNPs with an upper limit of only a few percent has been a serious hurdle. This is certainly true for biological applications where excitation power is restricted, and the upconversion quantum yield is thus even an order of magnitude lower. In recent years, large efforts have been devoted to improve the upconversion intensity of UCNPs. One strategy is to use a core/shell structure (such as $NaYF_4$:RE^{3+}@$NaYF_4$) where a shell of the same or similar material as the core is grown on the surface of the core.[20−27] This strategy aims to protect the excited activators—emitters, such as Er^{3+}, Tm^{3+} ions in the core, especially those near the surface—from nonradiative loss caused by surface defects and high-energy vibrational modes outside the particle. Our previous work[26,27] has already demonstrated that a large enhancement of the upconversion emission intensity can be achieved by such a core/shell structure.

However, a high upconversion yield does not guarantee high-quality performance in aforementioned FRET applications,

Received: July 8, 2011
Accepted: August 1, 2011
Published: August 02, 2011

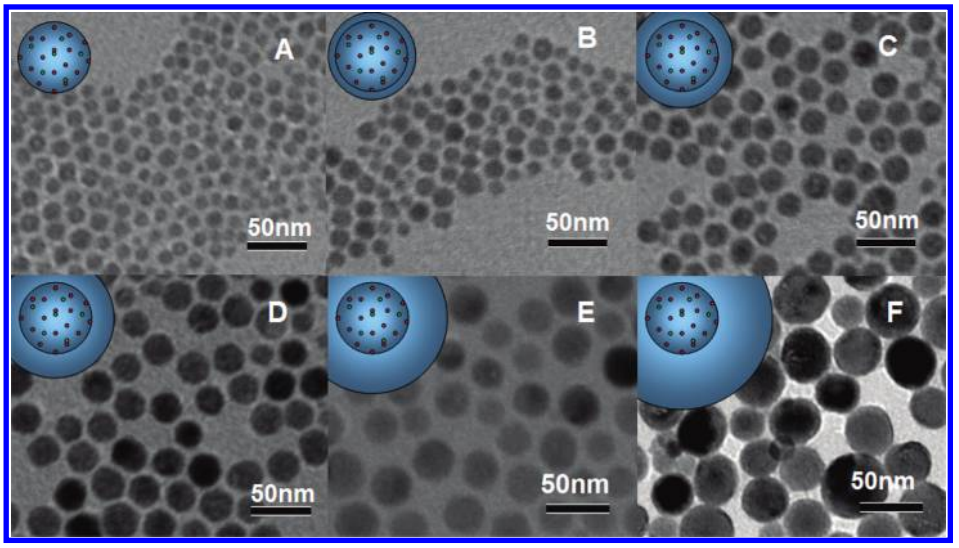

Figure 1. TEM results of six $NaYF_4$: Yb, Er@ $NaYF_4$ nanoparticle samples. Insets show a schematic illustration of the structures. (A): $NaYF_4$:20%Yb^{3+}, 2%Er^{3+} core UCNP. (B−F): core/shell structure $NaYF_4$:20%Yb^{3+},2%Er^{3+}@$NaYF_4$ UCNPs with different shell thicknesses as described in the text.

because the energy transfer efficiency from donor to acceptor could be impaired in the effort of enhancing upconversion luminescence. As is well-known, FRET is a nonradiative process where an excited state donor transfers its energy to a proximal ground state acceptor. The rate of energy transfer strongly depends on the distance between the donor and the acceptor. As far as the core/shell approach is concerned, a thick shell usually favors the upconversion luminescence within the saturation limit, whereas the distance between the donor (basically the core where emitters are located) and the acceptor (usually the organic molecules on the surface of the nanoparticle) becomes larger as the shell gets thicker. Therefore, for FRET application, the shell of the core/shell UCNPs can not be increased to such an extent that the strongest upconversion luminescence is reached.

In this work, core/shell structured $NaYF_4$:RE^{3+}@$NaYF_4$ UCNPs are introduced for the first time together with photosensitizing molecules to form a FRET model for PDT application. The relationship between the shell thickness and $^1O_2$ generation is studied in detail. The most important result is that there is an optimal value for the shell thickness, which corresponds neither to the thickness for which the strongest upconversion luminescence is reached nor to the thickness for which the highest energy transfer efficiency is obtained.

Strictly speaking, a so-called "FRET" process always accompanies reabsorption of the acceptor to the donor energy because the FRET requests overlap of the relevant spectra. In some cases, the two mechanisms can be distinguished from the emission kinetics of donor and acceptor, which is unfortunately not true for our case. In our case, the acceptor kinetics is always observed faster than that of the donor. In this work, the energy transfer efficiency is meant for a combination of both effects.

The core UCNPs and five core/shell structured UCNPs of different shell thicknesses were synthesized following a modified version of the well-known thermolysis method.[28,29] A schematic illustration of the six samples is given in Figure 1. Sample A is the $NaYF_4$:20%Yb^{3+},2%Er^{3+} core UCNP; samples B, C, D, E, and F have the same core as A but a different shell thickness, which was controlled during the synthesis. All of these six samples have good dispersibility in hexane. Figure 1 shows the transmission electron microscopy (TEM) images of the six hydrophobic samples. The average particle diameters are 16.0 nm (A), 20.2 nm (B), 23.0 nm (C), 27.4 nm (D), 34.4 nm (E), and 40.4 nm (F), corresponding to a shell thickness of 0 nm, 2.1 nm, 3.5 nm, 5.7 nm, 9.2 and 12.2 nm, respectively.

Overlap of the rose bengal (RB) absorption and UCNP emission spectra is shown in the Supporting Information, Figure S1. These spectra show that energy transfer between UCNP and RB can occur. The mechanism of FRET from UCNPs to RB photosensitizing molecules upon 980 nm excitation is shown in Figure 2. Absorption of pump photons populates the $^2F_{5/2}$ level of Yb^{3+}, which is followed by energy transfer from excited Yb^{3+} ions to Er^{3+} ions, populating the $^4I_{11/2}$ level of the latter. Higher electronic levels of Er^{3+}, such as the $^4F_{7/2}$ level, can then be populated by accepting the energy of another excited Yb^{3+} ion (energy transfer upconversion (ETU)), and by other processes, e.g., by direct absorption of another 980 nm photon (excited state absorption (ESA)), which are not as important as the ETU mechanism. Part of the $^4I_{11/2}$ excited ions relax to the $^4I_{13/2}$ level through multiphonon nonradiative relaxation. The $^4F_{7/2}$ level can decay nonradiatively to the $^2H_{11/2}$, $^4S_{3/2}$ and $^4F_{9/2}$ levels, leading to the green emission bands around 520 and 540 nm, and the red emission band at 650 nm. Another population route of the $^4F_{9/2}$ level is by absorption of a 980 nm photon or energy transfer from another Yb^{3+} ion from the $^4I_{13/2}$ level of the Er^{3+} ions. The absorption band (520−570 nm) of RB overlaps well with the green emission band of UCNPs. Therefore, if RB molecules are bound to the surface of UCNPs, one should be able to excite them indirectly by 980 nm light via UCNPs.

The integrated intensities of the upconversion emission of the six samples are shown in Figure 3a. This figure shows that the upconversion emission becomes monotonically stronger for thicker shells. We observe that upon binding with RB molecules, the green upconversion emission decreases for all samples, consistent with the energy transfer from the UCNP to photosensitizing molecules. The energy transfer efficiency of this process can be calculated from the quenching value of donor luminescent intensity given by $E = (I_D - I_{DA})/I_D$ where I_D and I_{DA} are emission intensities of the donor in the absence and presence of the acceptor, respectively.[30] The result is shown in Figure 3b. It is clear that for the bare core sample A-RB, 53% green emission is

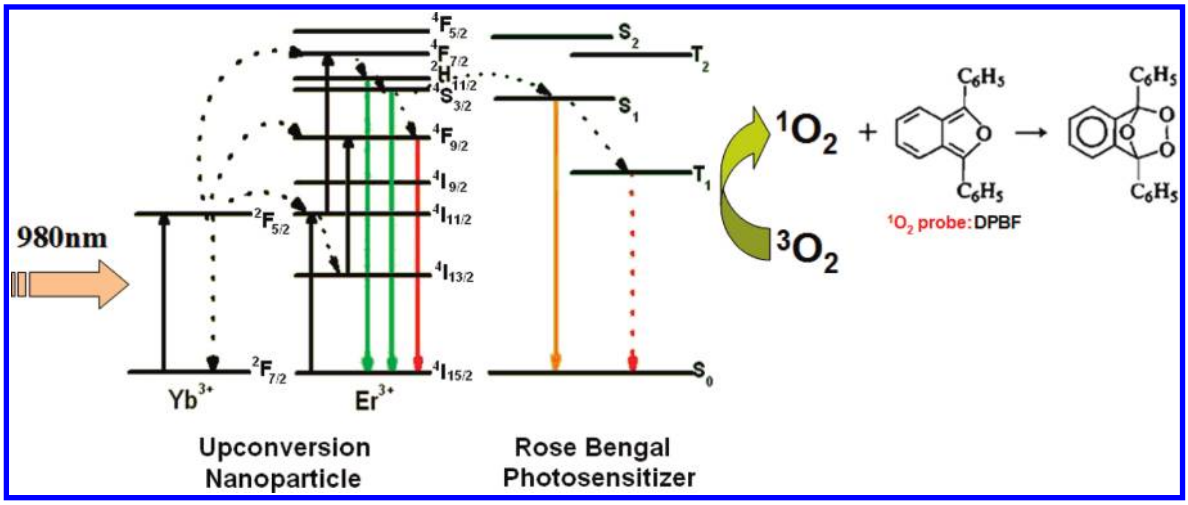

Figure 2. Mechanism of upconversion in the UCNP−RB nanoconjugate under excitation of 980 nm, and the oxidation reaction process of DPBF by $^1O_2$.

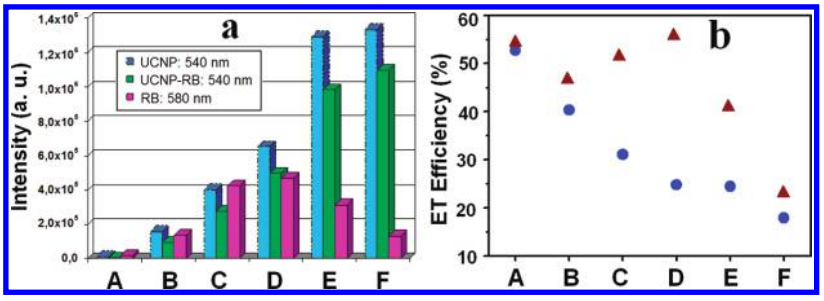

Figure 3. (a) 540 nm upconversion emission intensity of samples A−F before (blue columns) and after (green columns) RB attachment. Pink columns refer to the emission (580 nm) from RB, bound covalently to UCNPs. Excitation occurs by a CW diode laser at 980 nm with an excitation power of about 730 mW. (b) Energy transfer efficiency (E) of the six UCNP-RB samples (dot) as calculated based on the equation $E = (I_D - I_{DA})/I_D$ with details given in the text, FRET energy transfer efficiency defined as $E_{FRET} = 1 - \tau_{DA}/\tau_D$ is also given for the samples (triangle), where τ_{DA} is the lifetime of the donor in the presence of the acceptor. In the present case, it is equal to the RB fluorescence average lifetime.

quenched, which is in line with the fact that the upconversion emission centers (donors) and photosensitizer molecules (acceptors) are very close, leading to efficient energy transfer. For the core/shell structured upconversion samples, the efficiency decreases monotonically from around 40% for sample B to less than 18% for sample F.

Now we study the production of the final product. Singlet oxygen generation does not only depend on the aforementioned energy transfer efficiency. To study this in more detail, we monitored the fluorescence of RB in these samples (Figure 3a). As illustrated in Figure 2, the fluorescence of RB can be used to measure the efficiency of RB excitation, provided that $S_1 \rightarrow T_1$ intersystem crossing is about the same in the six samples. The results shown in Figure 3 demonstrate unambiguously that there exists an optimal shell thickness as far as the RB excitation is concerned. The samples **C**, **D**, and **E** are in this respect the best, with sample **D** showing the maximum emission. This means that a thinner or thicker shell is not efficient for exciting RB, even though a thin shell would favor energy transfer from nanoparticles to the photosensitizer. This "inconsistency" actually reflects the surface dependence of the photophysics of UCNPs. This is a typical feature of nanomaterials for which the surface is much more critical in determining their properties than for their bulk counterparts. In the present case, the upconversion quantum yield was enhanced with the increase of the shell thickness due to the better separation between the emitters in the core and surface related nonradiative de-excitation/quenchers. The shell thickness therefore has two opposite effects on the excitation of RB. On the one hand, a thick shell facilitates a strong upconversion emission, and thus favors excitation of RB. On the other hand, a thick shell is not favorable for the energy transfer efficiency, and thus excitation of RB will be reduced. Combination of these two opposing effects is thus indeed expected to lead to an optimum in the fluorescence of RB as a function of the shell thickness.

To verify that RB was indeed excited by NIR light via energy transfer from UCNPs in this covalently bound nanoparticle−photosensitizer conjugate, we have determined the temporal behavior of the emission from these samples. Figure 4 shows the time evolution of the 540 nm upconversion luminescence of the six UCNPs and the six UCNP-RB conjugates. Biexponential fits of the 540 nm emission decay led to the decay times listed in Table S1. From this table it can be seen that the decay times of 540 nm emission of UCNP-RB conjugates are shorter than those of corresponding UCNPs.

The fluorescence lifetime of RB is on the order of tens of picoseconds,[31] while the upconversion luminescence of Er^{3+} lasts much longer, usually (sub)microseconds. If RB is excited via energy transfer from UCNPs in the UCNP-RB conjugate, then the

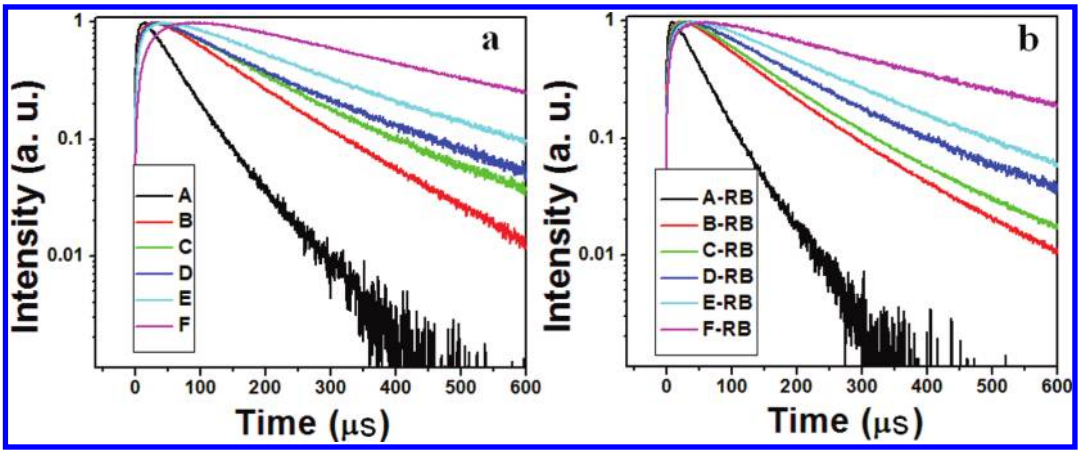

Figure 4. Temporal behavior of the 540 nm upconversion luminescence of the series of (A) UCNP samples A to F; (B) UCNP-RB conjugate samples A-RB to F-RB (λ_{ex} = 980 nm).

fluorescence of RB should be lengthened to the (sub)microsecond time scale. Figure S2 records the temporal behavior of the RB fluorescence at 580 nm for the six UCNP-RB conjugates, and demonstrates that indeed all the decays are extended to the microsecond regime. Figure S2 shows that the thicker the shell (from A to F), the longer the trace, exactly the same as observed for the temporal behavior of upconversion luminescence of UCNPs. Fits of the emission traces in Figure S2 to a biexponential function are given in Table S2. From this table it is clear that the microsecond rise component as well as the even longer decay component increase with the shell thickness. Thus fluorescence kinetics confirms that FRET occurs in UCNP-RB conjugates. However, more important information can be obtained when one looks into the details. The discrepancy between the emission kinetics of UCNPs at 540 nm and RB at 580 nm for UCNP-RB conjugates (Tables S1 and S2) may be related to the size distribution, which is more serious for larger samples, and luminescence center distribution in a single UCNP, which is more critical for small samples. Therefore, even for samples E (shell thickness ~9.2 nm) and F (shell thickness ~12.2 nm), where the nominal shell thicknesses are obviously larger than the reported FRET distance ~5−7 nm,[32,33] the kinetics of RB is still faster than that of UCNPs but in the similar order, indicating energy transfer occurs, which can be ascribed to the poor size distribution of larger samples of which a certain amount of UCNPs are still relatively small where FRET may occur. Another interesting phenomenon is that even for small samples (A−D), RB kinetics is always faster than UCNP kinetics, which can be understood from the distribution of the luminescence centers in a UCNP, where those in the center may be out of the effective distance for FRET. For these small samples, the kinetics of UCNPs is from two sorts of luminescence centers, i.e., those participate (short kinetics) and those do not participate (slow kinetics) in FRET process.

The generation of singlet oxygen is usually monitored by a chemical method using diphenylisobenzofuran (DPBF) as a probe.[34,35] When reacting with singlet oxygen, DPBF converts to its endoperoxide form. Therefore the decrease of the absorbance of DPBF can be used to determine the amount of singlet oxygen. Figure S3 in the Supporting Information shows the absorption spectra of ethanol solutions of DFBF and the six UCNP-RB conjugates as a function of exposure time to CW 980 nm irradiation. The main absorption band around 410 nm is due to DPBF, and the 560 nm absorption band is associated with RB. A UV−vis

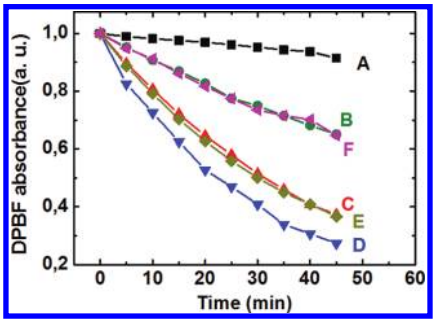

Figure 5. Absorbance at 410 nm of DPBF in ethanol solutions of A−F as a function of irradiation time. The excitation wavelength is 980 nm.

absorption spectrum of DPBF was taken every 5 min. For all samples, degradation of DPBF is observed.

Figure 5 displays the absorbance of DPBF at 410 nm versus exposure time. The rate at which the intensity falls off as a function of time is roughly proportional to the efficiency with which singlet oxygen is generated.[36−38] It is readily seen that UCNP-RB conjugates C, E, and in particular D are the best in generating singlet oxygen. Thus, nanoparticles with a 16 nm core and a 6 nm shell are the best in generating $^1O_2$, although these particles show neither the strongest upconversion luminescence nor the highest energy transfer efficiency.

We have studied UCNPs for FRET application with a model system of $NaYF_4$:Yb^{3+}, Er^{3+}@$NaYF_4$. From singlet oxygen generation and photophysics of UCNP−photosensitizer conjugates, it is verified that the best shell thickness for the performance of the FRET conjugates, which is for the highest yield of $^1O_2$ generation in the present case, results in neither the highest upconversion luminescence, nor the highest FRET efficiency. The actual optimal shell thickness should be acceptor and core size relevant. Our results shall be helpful in exploring more efficient FRET devices based on nanomaterials.

■ ASSOCIATED CONTENT

Supporting Information. Experimental section, Figures S1−S3, and Tables S1 and S2. This material is available free of charge via the Internet at http://pubs.acs.org

AUTHOR INFORMATION

Corresponding Author

*(H.Z.) Tel: +31-20-5256976; e-mail: h.zhang@uva.nl. (X.K.) Tel: +86-431-86176313; e-mail: xgkong14@ciomp.ac.cn.

ACKNOWLEDGMENT

This work was supported by the Innovation Research Program (IOP) grant of The Netherlands, the exchange program between CAS of China and KNAW of The Netherlands, the Joint Ph.D. training program between CAS and KNAW, and NSFC of China (60771051, 60601015, 10674132, 10874179 and 20603035).

REFERENCES

(1) Wang, L.; Yan, R.; Huo, Z.; Wang, L.; Zeng, J.; Bao, J.; Wang, X.; Peng, Q.; Li, Y. Fluorescence Resonant Energy Transfer Biosensor Based on Upconversion-Luminescent Nanoparticles. *Angew Chem., Int. Ed.* **2005**, *44*, 6054–6057.

(2) Wang, M.; Hou, W.; Mi, C. C.; Wang, W. X.; Xu, Z. R.; Teng, H. H.; Mao, C. B.; Xu, S. K. Immunoassay of Goat Antihuman Immunoglobulin G Antibody Based on Luminescence Resonance Energy Transfer between Near-Infrared Responsive $NaYF_4$:Yb,Er Upconversion Fluorescent Nanoparticles and Gold Nanoparticles. *Anal. Chem.* **2009**, *81*, 8783–8789.

(3) Rantanen, T.; Päkkilä, H.; Jämsen, L.; Kuningas, K.; Ukonaho, T.; Lövgren, T.; Soukka, T. Tandem Dye Acceptor Used To Enhance Upconversion Fluorescence Resonance Energy Transfer in Homogeneous Assays. *Anal. Chem.* **2007**, *79*, 6312–6318.

(4) Bednarkiewicz, A.; Nyk, M.; Samoc, M.; Strek, W. Up-conversion FRET from Er^{3+}/Yb^{3+}:$NaYF_4$ Nanophosphor to CdSe Quantum Dots. *J. Phys. Chem. C* **2010**, *114*, 17535–17541.

(5) Guo, H. C.; Idris, N. M.; Zhang, Y. LRET-Based Biodetection of DNA Release in Live Cells Using Surface-Modified Upconverting Fluorescent Nanoparticles. *Langmuir* **2011**, *27*, 2854–2860.

(6) Rantanen, T.; Järvenpää, M. L.; Vuojola, J.; Kuningas, K.; Soukka, T. Fluorescence-Quenching-Based Enzyme-Activity Assay by Using Photon Upconversion. *Angew Chem., Int. Ed.* **2008**, *47*, 3811–3813.

(7) Jiang, S.; Zhang, Y. Upconversion Nanoparticle-Based FRET System for Study of siRNA in Live Cells. *Langmuir* **2010**, *26*, 6689–6694.

(8) Wang, L. Y.; Yan, R. X.; Huo, Z. Y.; Wang, L.; Zeng, J. H.; Bao, J.; Wang, X.; Peng, Q.; Li, Y. D. Fluorescence Resonant Energy Transfer Biosensor Based on Upconversion-Luminescent Nanoparticles. *Angew Chem., Int. Ed.* **2005**, *44*, 6054–6057.

(9) Kuningas, K.; Ukonaho, T.; Päkkilä, H.; Rantanen, T.; Rosenberg, J.; Lövgren, T.; Soukka, T. Upconversion Fluorescence Resonance Energy Transfer in a Homogeneous Immunoassay for Estradiol. *Anal. Chem.* **2006**, *78*, 4690–4696.

(10) Chen, Z. G.; Chen, H. L.; Hu, H.; Yu, M. X.; Li, F. Y.; Zhang, Q.; Zhou, Z. G.; Yi, T.; Huang, C. H. Versatile Synthesis Strategy for Carboxylic Acid-Functionalized Upconverting Nanophosphors as Biological Labels. *J. Am. Chem. Soc.* **2008**, *130*, 3023–3029.

(11) Li, Z. Q.; Zhang, Y.; Jiang, S. Multicolor Core/Shell-Structured Upconversion Fluorescent Nanoparticles. *Adv. Mater.* **2008**, *20*, 4765–4769.

(12) Klostermeier, D.; Sears, P.; Wong, C. H.; Millar, D. P.; Williamson, J. R. A Three-Fluorophore FRET Assay for High-Throughput Screening of Small-Molecule Inhibitors of Ribosome Assembly. *Nucleic Acids Res.* **2004**, *32*, 2707.

(13) Jares-Erijman, E. A.; Jovin, T. M. FRET Imaging. *Nat. Biotechnol.* **2003**, *21*, 1387–1395.

(14) Prasad, P.N.; *Introduction to Biophotonics*; Wiley-Interscience: New York, 2003.

(15) Samia, A. C. S.; Chen, X. B.; Burda, C. Semiconductor Quantum Dots for Photodynamic Therapy. *J. Am. Chem. Soc.* **2003**, *125*, 15736.

(16) Bakalova, R.; Ohba, H.; Zhelev, Z.; Ishikawa, M.; Baba, Y. Quantum Dots As Photosensitizers? *Nat. Biotechnol.* **2004**, *22*, 1360.

(17) Chatterjee, D. K.; Zhang, Y. Upconverting Nanoparticles as Nanotransducers for Photodynamic Therapy in Cancer Cells. *Nanomedicine* **2008**, *3*, 73–82.

(18) Qian, H. S.; Guo, H. C.; Ho, P. C. L.; Mahendran, R.; Zhang, Y. Mesoporous-Silica-Coated Up-Conversion Fluorescent Nanoparticles for Photodynamic Therapy. *Small* **2009**, *5*, 2285–2290.

(19) Guo, H. C.; Qian, H. S.; Idris, N. M.; Zhang, Y. Singlet Oxygen-Induced Apoptosis of Cancer Cells Using Upconversion Fluorescent Nanoparticles as a Carrier of Photosensitizer. *Nanomed.: Nanotechnol., Biol. Med.* **2010**, *6*, 486–495.

(20) Mai, H. X.; Zhang, Y. W.; Sun, L. D.; Yan, C. H. Highly Efficient Multicolor Up-Conversion Emissions and Their Mechanisms of Monodisperse $NaYF_4$:Yb,Er Core and Core/Shell-Structured Nanocrystals. *J. Phys. Chem. C* **2007**, *111*, 13721–13729.

(21) Yi, G. S.; Chow, G. M. Water-Soluble $NaYF_4$:Yb,Er(Tm)/$NaYF_4$/Polymer Core/Shell/Shell Nanoparticles with Significant Enhancement of Upconversion Fluorescence. *Chem. Mater.* **2007**, *19*, 341–343.

(22) Boyer, J. C.; Gagnon, J.; Cuccia, L. A.; Capobianco, J. A. Synthesis, Characterization, and Spectroscopy of $NaGdF_4$: Ce^{3+}, Tb^{3+}/$NaYF_4$ Core/Shell Nanoparticles. *Chem. Mater.* **2007**, *19*, 3358–3360.

(23) Schafer, H.; Ptacek, P.; Zerzouf, O.; Haase, M. Synthesis and Optical Properties of KYF_4/Yb, Er Nanocrystals, and their Surface Modification with Undoped KYF_4. *Adv. Funct. Mater.* **2008**, *18*, 2913–2918.

(24) Qian, H. S.; Zhang, Y. Synthesis of Hexagonal-Phase Core—Shell $NaYF_4$ Nanocrystals with Tunable Upconversion Fluorescence. *Langmuir* **2008**, *24*, 12123–12125.

(25) Wang, F.; Wang, J.; Liu, X. G. Direct Evidence of a Surface Quenching Effect on Size-Dependent Luminescence of Upconversion Nanoparticles. *Angew. Chem., Int. Ed.* **2010**, *49*, 7456–7460.

(26) Wang, Y.; Tu, L. P.; Zhao, J. W.; Sun, Y. J.; Kong, X. G.; Zhang, H. Upconversion Luminescence of β-$NaYF_4$: Yb^{3+}, Er^{3+}@β-$NaYF_4$ Core/Shell Nanoparticles: Excitation Power Density and Surface Dependence. *J. Phys. Chem. C* **2009**, *113*, 7164–7169.

(27) Wang, Y.; Smolark, S.; Kong, X. G.; Buma, W. J.; Brouwer, A. M.; Zhang, H. Effect of Surface Related Organic Vibrational Modes in Luminescent Upconversion Dynamics of Rare Earth Ions Doped Nanoparticles. *J. Nanosci. Nanotechnol.* **2010**, *10*, 7149–7153.

(28) Boyer, J. C.; Vetrone, F.; Cuccia, L. A.; Capobianco, J. A. Synthesis of Colloidal Upconverting $NaYF_4$ Nanocrystals Doped with Er^{3+}, Yb^{3+} and Tm^{3+}, Yb^{3+} via Thermal Decomposition of Lanthanide Trifluoroacetate Precursors. *J. Am. Chem. Soc.* **2006**, *128*, 7444–7445.

(29) Yi, G. S.; Chow, G. M. Synthesis of Hexagonal-Phase $NaYF_4$:Yb,Er and $NaYF_4$:Yb,Tm Nanocrystals with Efficient Up-Conversion Fluorescence. *Adv. Funct. Mater.* **2006**, *16*, 2324–2329.

(30) Lakowicz, J.R.; *Principles of Fluorescence Spectroscopy*, 2nd ed.; Kluwer Academic: New York, 1999.

(31) Rodgers, M. A. J. Picosecond Fluorescence Studies of Rose Bengal in Aqueous Micellar Dispersions. *Chem. Phys. Lett.* **1981**, *78*, 509–514.

(32) Wuister, S. F; Donegá, C. D. M.; Meijerink, A. Efficient Energy Transfer Between Nanocrystalline YAG:Ce and TRITC. *Phys. Chem. Chem. Phys.* **2004**, *6*, 1633.

(33) Tian, L. J.; Sun, Y. J.; Yu, Y.; Kong, X. G.; Zhang, H. Surface Effect of Nano-Phosphors Studied by Time-Resolved Spectroscopy of Ce^{3+}. *Chem. Phys. Lett.* **2008**, *452*, 188.

(34) Spiller, W.; Kliesch, H.; Wohrele, D.; Hackbarth, S.; Roder, B.; Schnurpfeil, G. J. Singlet Oxygen Quantum Yields of Different Photosensitizers in Polar Solvents and Micellar Solutions. *J. Porphyrins Phthalocyanines* **1998**, *2*, 145.

(35) Tada, D. B.; Vono, L. L. R.; Duarte, E. L.; Itri, R.; Kiyohara, P. K.; Baptista, M. S.; Rossi, L. M. Methylene Blue-Containing Silica-Coated Magnetic Particles: A Potential Magnetic Carrier for Photodynamic Therapy. *Langmuir* **2007**, *23*, 8194–8199.

(36) Wang, S.; Gao, R.; Zhou, F.; Selke, M. Nanomaterials and Singlet Oxygen Photosensitizers: Potential Applications in Photodynamic Therapy. *J. Mater. Chem.* **2004**, *14*, 487–493.

(37) Ohulchanskyy, T. Y.; Roy, I.; Goswami, L. N.; Chen, Y.; Bergey, E. J.; Pandey, R. K.; Oseroff, A. R.; Prasad, P. N. Organically Modified Silica Nanoparticles with Covalently Incorporated Photosensitizer for Photodynamic Therapy of Cancer. *Nano Lett.* **2007**, *7*, 2835–2842.

(38) Roy, I.; Ohulchanskyy, T. Y.; Pudavar, H. E.; Bergey, E. J.; Oseroff, A. R.; Morgan, J.; Dougherty, T. J.; Prasad, P. N. Ceramic-Based Nanoparticles Entrapping Water-Insoluble Photosensitizing Anticancer Drugs: A Novel Drug-Carrier System for Photodynamic Therapy. *J. Am. Chem. Soc.* **2003**, *125*, 7860–7865.